FORSCHUNGSZENTRUM
ROSSENDORF e.V.

FZR

FZR 93 - 09
April 1993
Preprint

B. Kämpfer, O.P. Pavlenko

Photon production in an expanding gluon-enriched plasma

Photon production in an expanding gluon-enriched plasma

B. KÄMPFER[a,b], O.P. PAVLENKO[a,c]

[a]Research Center Rossendorf, Institute for Nuclear and Hadron Physics
PF 19, O-8051 Dresden, Germany
[b]Inst. Theor. Phys. (KAI e.V.), TU Dresden, Germany
[c]Institute for Theoretical Physics, Kiev, Ukraine

Abstract

Photon production in an expanding gluon plasma with initially little quark admixture is considered. Photons are created by lowest order α_s processes which include quarks. Chemical equilibration of the quarks in turn is followed by rate equations which rely on lowest order α_s $gg \rightleftharpoons q\bar{q}$ processes. Expansion slows down the quark cooking. Compared with the standard local equilibrium estimates we find a drastic reduction of medium-energy photons if the initial quark admixure is below 20% of the chemical saturation density. Higher initial temperatures increase significantly the high-energy photon yield and overcompensate this reduction.

1 Introduction

Future ultra-relativistic heavy-ion experiments, such as the lead beam project at CERN-SPS, or the RHIC project, or the LHC plan, are aimed to search for deconfinement effects in dense and hot nuclear matter. The corresponding theoretical predictions are mainly based on lattice QCD calculations [1], which are addressed at present to equilibrium (thermal, chemical, and mechanical) properties of the quark-gluon plasma. Various estimates indeed point to the possibility to achieve local equilibrium.

In the very first reaction stage of the colliding nuclei there are hard parton scatterings which produce a part of secondaries, e.g., in mini-jets [2]. Due to semi-hard interactions the partons evolve towards local equilibrium, however, in strong competition with the rapid (mainly longitudinal) expansion of the matter. Semi-hard scatterings in parton matter can be in principle be calculated within the framework of perturbative QCD. Perturbative cross sections for gluon-gluon interaction are larger than the ones for quark-quark or quark-gluon scatterings. This fact might imply that in ultra-relativistic heavy-ion collisions probably a gluon plasma is initially created with only a few quarks admixed [3, 4]. Present parton cascade models support such a picture [5, 6, 7, 8, 9]. The large gluon-gluon cross section helps to thermalize the gluon system fastly. In a second reaction stage the few quarks and the gluons thermalize. Even being early in thermal equilibrium such a gluon plasma with quark admixture is still in a chemical off-equilibrium state for some time. On a larger, third time scale the chemical equilibration proceeds. This is another facet of the deconfinement physics. Since many of the proposed probes of the quark-gluon plasma rely on indirect measurements of the deconfined quark matter distribution it seems to be necessary to refine the standard estimates (cf. [10]) which rely on chemical equilibrium.

The aim of our paper is to analyse the direct photon production (cf. [11] and Refs. quoted therein) in a rapidly expanding gluon plasma, which is initially in thermal equilibrium (also with the quark admixture), and which equilibrates towards chemical equilibrium by quark production in the above outlined three-stage scenario. The chemical equilibration process occupies thereby the largest space-time volume. For some intermediate photon energy (≈ 2 GeV) this stage might be the most important one. Earlier and "hotter" stages probably produce harder photons, while softer photons emerge mainly from the confinement era and later.

The NA34 and WA80 photon measurements at previous SPS oxygen and sulphur runs indicate that the photon spectra are determined by hadronic (π^0's) decays at least up to 95% [12]. Recent experimental refinements seem to leave in the region $p_\perp = 1$ - 2 GeV some yield which is not yet explained by hadronic decays [13]. While a careful confirmation of this result is still needed, such improved measurements are encouraging with respect to the direct photons. Also in view on future experiments one needs more detailed estimates of the direct photon spectra to get some hints where thermal photons show up most clearly and might be identified experimentally. Also the relation of photons from hot hadron matter and those of the plasma needs more investigations.

Our paper is organized as follows. In section 2 we consider the chemical quark equilibration process. We use the results in section 3 then to analyze the photon yield from the equilibrating plasma. We also make a clue to the modified dilepton production which measures largely the quark content of the plasma too. The summary can be found in section 4.

2 Evolution of quark degrees of freedom

We employ a transport model of coupled Boltzmann type equations for the parton distribution functions $f_a(p, x)$, where the subscript $a = g, q, \bar{q}$ denotes the parton species,

$$p^\mu \partial_\mu f_a(p, x) = \mathcal{C}_a(p, x) \tag{1}$$

with Lorentz invariant collisional term for the binary $2 \to 2$ processes $ab \to cd$

$$\mathcal{C}_a(p_a, x) = -\frac{1}{2(1+\delta_{ab})(1+\delta_{cd})} \int d\Gamma_b d\Gamma_c d\Gamma_d (f_a f_b - f_c f_d) \times \tag{2}$$

$$(2\pi)^4 \delta^{(4)}(p_a + p_b - p_c - p_d) \sum |\mathcal{M}_{ab\to cd}|^2.$$

Here $p = (E, \vec{p})$ is the parton's four momentum, $x = (t, \vec{r})$ is the space-time, $d\Gamma = d^3\vec{p}/(2\pi)^3 2E$ denotes the momentum space volume element, and $\sum |\mathcal{M}|^2$ stands for the lowest order α_s squared matrix elements which are summed over spin and colour. The distribution is normalized by the parton density $g_a \int d^3\vec{p}(2\pi)^{-3} f_a(p, x) = n_a(x)$, where g_a denote the degeneracy factors.

In general one has to sum over various reaction channels in the collisional term (2), but we consider here the $gg \rightleftharpoons q\bar{q}$ reactions as most important for changing the quark-gluon composition (the parton number changing processes $gg \rightleftharpoons ggg$ are considered in Ref. [9]). The corresponding t channel reactions do not change the parton species numbers, however, are important to maintain the thermal equilibrium. We follow the evolution of the parton system after thermalization according to the estimates [4] within perturbative QCD.

We do not consider $1 \rightleftharpoons 2$ reactions with partons "1" with high virtuality [6, 7] since for near-mass shell partons in thermal equilibrium such reactions are expected to be suppressed. In addition such reactions would introduce a term $\propto n$ in the below derived rate equations, which can be neglected in comparison with the quadratic terms in case of high parton density.

The expression (2) might be improved by taking into account higher order perturbative corrections and also non-perturbative soft parton reactions [14]. Since we focus on the early plasma stages, wherein the medium-heavy probes are cooked out, and on qualitative features, for our explorative study the first-order perturbative estimates might serve as some useful reference value. Even though the early stages occupy only a comparatively small region of the space-time region of matter evolution, it plays an important rôle for many experimental signals [10].

Relying on the assumption of the boost invariant longitudinal expansion of the parton matter, eq. (1) can be rewritten as

$$(\partial_\tau - \frac{\text{th}\xi}{\tau}\partial_\xi) f_a = \frac{1}{E_a}\mathcal{C}_a \tag{3}$$

where $\tau = \sqrt{t^2 - z^2}$ is the proper time (z is the longitudinal coordinate and t the time in cms); $\xi = \eta - y$, with η and y as space-time and parton rapidity, respectively. Intergrating eq. (3) over momentum space $(d^3p_a/(2\pi)^3)$ results in the parton density evolution equation

$$\frac{dn_a}{d\tau} + \frac{n_a}{\tau} = \int d\Gamma_a \mathcal{C}_a. \tag{4}$$

The right hand side can be transformed into an expression often used in kinetic theory approaches

$$\int d\Gamma_a \mathcal{C}_a = -\frac{1}{2(1+\delta_{ab})(1+\delta_{cd})} \int_{4m^2}^{\infty} ds \; [\int \frac{d^3p_a}{(2\pi)^3}\frac{d^3p_b}{(2\pi)^3} f_a f_b v_{ab} \tilde{\sigma}(s) \delta(s - (p_a+p_b)^2)$$
$$- \int \frac{d^3p_c}{(2\pi)^3}\frac{d^3p_d}{(2\pi)^3} f_c f_d v_{cd} \tilde{\sigma}(s) \delta(s - (p_c+p_d)^2)], \tag{5}$$

where the cross section is defined as

$$\tilde{\sigma}(s) = \int_{t_-}^{t^+} \sum |\mathcal{M}(s,t)|^2 \, dt, \quad t_\pm = m^2 - \frac{s}{2}(1 \pm W(s)), \quad W(s) = \sqrt{1 - 4m^2/s}, \tag{6}$$

and $v_{ab,cd}$ denote the relative flux velocities. The parameter m is introduced here as cut-off for the infrared divergent cross sections $gg \to q\bar{q}$ and will be discussed below. Note that $\tilde{\sigma}$ in eq. (5) is not averaged, as usual, over the number of initial states of the colliding partons [15].

According to our propositions on thermal equilibrium we approximate the momentum space distribution by a Maxwellian, i.e., $f_a \approx f_a^{eq} = \lambda_a(\tau) \exp\{-E_a/T(\tau)\}$ with the weight factor λ_a and unique temperature T. λ_a resembles the fugacity. In chemical off-equilibrium the weights need to be determined dynamically. In chemical equlibrium $\lambda_a = 1$ for all a.

Using the energy conservation (that is the energy weighted integration over eq. (1)) one recovers the known solution for the temperature $T(\tau) \propto \tau^{-1/3}$. That means the chemical off-equilibrium does not affect the thermal history as long as thermal equilibrium is maintained.

With the ansatz $f_a = f_a^{eq}$ in the collisional term (5) and with the dynamical equations (4) one gets a closed system of equations for the parton species densities $n_a(\tau)$. For our purpose it is convenient to introduce the total parton density $n = n_g + n_q + n_{\bar{q}}$ and the relative gluon weight $x(\tau) = n_g(\tau)/n(\tau)$; $1 - x$ is the total quark weight. Then eqs. (4, 5) can be cast in the form

$$\frac{dn}{d\tau} = -\frac{\gamma n}{\tau}, \quad \frac{dx}{d\tau} = n\mathcal{R}(\beta[1-x]^2 - x^2), \tag{7}$$

$$\mathcal{R} = \frac{2\pi\alpha_s^2}{3m^2}\left(\frac{m}{T}\right)^5 I(m,T), \quad I(m,T) = \int_2^\infty dz z^2 \tilde{\sigma}(z) K_1(\frac{mz}{T}),$$

$$\tilde{\sigma}(z) = (1 + 4z^{-2} + z^{-4}) \,\mathrm{arth} W - (7 + 3z^{-2})W/8, \quad W(z) = \sqrt{1 - 4z^{-2}}$$

($\beta = 4/9$ for u, d quarks; $\gamma = 1$ for the Bjorken scenario, and $\gamma = 0$ switches off any expansion). The expression for the cross section $\tilde{\sigma}$ is derived from the standard cross section for the reaction $gg \to q\bar{q}$ [16].

If the above introduced cut-off parameter m is identified with the thermal quark mass according to screening effects within perturbative QCD, i.e., $m(T) = \sqrt{2\pi\alpha_s/3}T$ [17], then the system (7) can be solved analytically for constant α_s

$$n(\tau) = n_0\left(\frac{\tau_0}{\tau}\right)^\gamma, \quad x(\tau) = \frac{(\beta+\sqrt{\beta})A_+ - \varphi(\tau)(\beta-\sqrt{\beta})A_-}{(\beta-1)(A_+ - \varphi(\tau)A_-)}, \tag{8}$$

$$A_\pm = (\beta-1)x_0 - \beta \pm \sqrt{\beta}, \quad \varphi(\tau) = \exp\{\tau_Q[\left(\frac{\tau}{\tau_0}\right)^{1-\gamma/3} - 1]\}$$

$$\tau_Q = \frac{3}{\pi}(1-\frac{\gamma}{3})^{-1}\sqrt{\beta}n_0\tau_0T_0^{-2}\kappa^7 I(\kappa), \quad \kappa = \sqrt{2\pi\alpha_s/3}$$

$$I(\kappa) = \int_2^\infty dz z^2\tilde{\sigma}(z)K_1(\kappa z) \quad (\approx 10^{3.32-5.15\kappa+1.5\kappa^2} \text{ for } \alpha_s < 1),$$

($\hbar = c = 1$). The results of calculations of the quark weight $1-x$ are displayed in Fig. 1 for the set of initial parameters $x_0 = 0.8$ and 1, $n_0 = 10$ fm^{-3}, $T_0 = 500$ MeV, $\tau_0 = 0.5$ fm/c, $\kappa = 1.1$. There are quite different estimates of such initial parameters for RHIC and LHC conditions, respectively [4, 7, 9, 18]. The appropriate choice of these initial parameters is still matter of debate. The authors of Refs. [4, 7] claim high parton density of the gluon-enriched plasma. Otherwise, the HIJING model [9] points to a strongly diminished (with respect to phase space saturation) initial parton density. One can see in Fig. 1 that it needs a rather long time for cooking out the quarks in the longitudinally expanding plasma. This is in line with the model [9], where also a slow chemical relaxation is found; however, smaller parton densities (but not temperature) are used. We conclude that after $\tau/\tau_0 \approx 5\tau_Q^{-1}$ the quarks are approximately in local chemical equilibrium, i.e., $x \to x_{eq} = 2/5$, rather independent on the initial weight (cf. Fig. 1).

There are two reasons for the slow chemical quark equilibration. First, quark cooking depends sensitively on the density of gluons, which is decreasing due to expansion. Indeed, when neglecting the expansion, one approaches faster to equilibrium (cf. dashed curve in Fig. 1). Second, the quark screening mass here introduced also prevents fast chemical equilibration at initial high temperatures. This is in accordance with previous rough estimates [4], in which, however, the expansion has been neglected. For our rather conservative parameter set we get $\tau_Q = 0.42$ (at $\alpha_s = 0.5$). One can easily check the variations of τ_Q when changing the intial parameters by means of the transparent equations (8). E.g. the dotted curve in Fig. 1 displays chemical equilibration for $\tau_Q = 0.1$, which might be realized by strong under-saturation of initial parton density as used in Ref. [9]. Probably soft and higher order processes increase the quark production. In addition there might be inelastic gluon producing processes, such as included in Ref. [9], which prevent the too fast dilution of the expanding parton system due to expansion. Then the parton density stays higher, and accordingly more quarks can be produced.

3 Photon production

Now we use the above evolution of the chemical composition of the plasma to calculate the photon production. We follow the standard approaches [11] and use the quark -antiquark annihilation $q\bar{q} \to g\gamma$ and Compton like processes $gq(\bar{q}) \to q(\bar{q})\gamma$. The lowest order

α_s contributions are [20]

$$\frac{dN_\gamma^{Comp}}{d^4x d^3p/E} = \frac{10\alpha\alpha_s}{9\pi^4} T^2 \mathrm{e}^{-E/T} \{\log(\frac{4ET}{k_c^2}) + \frac{1}{2} - C_E\} \lambda_q \lambda_g, \tag{9}$$

$$\frac{dN_\gamma^{annih}}{d^4x d^3p/E} = \frac{10\alpha\alpha_s}{9\pi^4} T^2 \mathrm{e}^{-E/T} \{\log(\frac{4ET}{k_c^2}) - 1 - C_E\} \lambda_q^2, \tag{10}$$

where $(E, \vec{p})$ denotes here the photon's four momentum, k_c is an infrared cut-off, and $C_E \approx 0.577$ stands for the Euler constant. The relative weights $\lambda_{g,q}$ are connected with the gluon weight x via

$$\lambda_q = \frac{(1-x)n}{T^3}\frac{\pi^2}{24}, \quad \lambda_g = \frac{xn}{T^3}\frac{\pi^2}{16}, \tag{11}$$

where u,d quarks are included.

In Ref. [20] the resummation technique of Braaten and Pisarski [21] has been used to regularize infrared divergences in the rates (9, 10). However, in our case of chemical off-equilibrium gluon plasma the problem of the divergences needs special consideration, in general. Since we focus here on not too soft photons with $E > T$, the photon emission turns out to dependend on k_c not too sensitively. We follow therefore a variant in Ref. [20] and choose $k_c^2 = 2m_q^2 = \frac{4\pi\alpha_s}{3}T^2$.

Combining then eqs. (9 - 11) one gets for the total photon rate

$$\frac{dN}{d^4x\, d^3p/E} = \frac{5\alpha\alpha_s n^2}{72^2 T^4} \mathrm{e}^{-E/T} \{[\log(\frac{3E}{\pi\alpha_s T}) - C_E](2 - x - x^2) - \frac{1}{2}(4 - 11x + 7x^2\}. \tag{12}$$

The effect of incomplete chemical equilibration might be discussed by using the ratio $\xi = N(x)/N(x_{eq})$. Assuming first the same T, n for both the equilibrated and non-equilibrated sources, we get, e.g., $\xi = 0.5$ for x = 0.8 and $\xi = 0.2$ for x = 0.95 at $E \sim$ 2 GeV and $\alpha_s = 0.5$ and $T = 500$ MeV (cf. Fig. 2). Smaller photon energies ($E \sim 1$ GeV) result in slightly higher values of ξ at $x > x_{eq}$, while higher photon energies ($E \sim 3$ GeV) reduce ξ. Note that below $E \sim 1$ GeV the used formula for the rate is not longer reliable [20], as seen in the overshoot in the region $x = x_{eq} \cdots 0.7$. At $E > 1$ GeV the α_s dependence is negligible, as the temperature dependence too. In this comparison we assume full gluon phase space population, i.e., $n_{sat} \approx 40\pi^{-2}T^3$. In Ref. [9] a strongly reduced early parton number is found within the HIJING prediction, $n < 0.2 n_{sat}$. This would reduce the rate additionally to 5% of the above values. Here we follow more the prediction of Refs. [4, 7] which point to early gluon phase space saturation. Therefore, the influence of the chemical quark off-equilibrium effect is within a factor $\frac{1}{2}$ as long as initially in the gluon plasma the quark admixture is above 20% (i.e., $x \leq 0.85$). If the primordial quark content is less, then a dramatic reduction of the thermally produced hard photons from the deconfined plasma appears. at least in lowest order α_s processes, see Fig. 2.

The time integrated rate

$$\frac{dN}{dy\, d^3p/E} = \pi R^2 \int d\tau\, \tau \frac{dN}{dy\, d^3p/E} \tag{13}$$

(R is the transverse radius of the plasma) is displayed in Fig. 3. Please note that we use in Fig. 3 the scaled rate (13) in units of $n_0^2/T_0^6 R^2$, i.e., initial gluon phase space suppression would strongly reduce the actual yield as discussed above. Let us first consider the reference case $x = x_{eq}$, i.e., chemical equilibrium. There is a conservative estimate $\tau_0 = 1$ fm/c and $T_0 = 300$ MeV [18]. Assuming no strong entropy production in the subsequent evolution, these values fix the final hadron rapidity density. Shorter initial times, as advovated in Refs. [4, 7, 9, 19] result in higher initial temperatures at this fixed rapidity density, e.g., $(\tau_0, T_0) =$ (0.3 fm/c, 448 MeV) or (0.1 fm/c, 646 MeV). One observes in Fig. 3 that higher initial temperatures and shorter initial times increase considerably the high-energy photon yield. For the low-energy photons the rates (9, 10) are not reliable, but nevertheless only a small effect is seen. That is because the early hot stages produce the harder photons. For indicating the sensitivity of the yield we also use other initial values, which belong to different hadron rapidity densities, such as (0.5 fm/c, 300 MeV) and (1 fm/c, 500 MeV). α_s variations are demonstrated in Fig. 3 too; the effect in the scaled yield is of minor importance. The upper part in Fig. 3 displays the effect of incomplete chemical quark equilibration. In case of small values of $\tau_Q < 0.1$ one recovers the overall suppression by a factor 0.5 for $x_0 = 0.8$. Assuming a faster quark equilibrating process, described by larger τ_Q, then the low-energy photons are not longer suppressed while the high-energy photons are, because in later stages where quarks are in equilibrium the high-energy photon production is not effective. Nevertheless the net effect is not too large. The main suppression can arise from intial gluon phase space under-saturation.

Finally we comment on the dilepton yield. Also the dilepton production rate is related to the quark density. Therefore, a modification of the lowest order α_s processes is to be expected in the initially gluon-enriched plasma too. This modification is similar to the above presented one. The photon yield can be cast into the form

$$\frac{dN}{d^2p_\perp\, dy} = \frac{15}{5184}\alpha\alpha_s \pi R^2 \sqrt{2\pi}\frac{(n_0\tau_0)^2}{p_\perp^4}\int_{p_\perp/T_0}^{p_\perp/T_f} dz z^{5/2} e^{-z} F(x,z), \tag{14}$$

where $F(x,z)$ is the expression in paranthesis in eq. (12) but with the replacement E/T by z, which is weakly dependent on z. The dilepton yield for the lowest order $\alpha\alpha_s$ processes are similar. In equlibrium $n_0 \propto T_0^3$, therefore, both rates depend essentially on the squared hadron rapidity density $dN_h/dy \propto T_0^3\tau_0$. However, if $n < n_{sat}$ then the same additional reduction of the dilepton rate appears as discussed above for photons.

To estimate the net effect of the slow quark equilibration we mention that of course softer processes probably enhance at later times the production rates. Nevertheless, if the picture as forcast in Refs. [3, 4] and supported by parton cascading is correct and initially a gluon plasma is created, then the early deconfinement probes, which measure rather directly the thermalized quark distribution, are expected to be suppressed. This is not necessarily a bad effect, since there are speculations [22] that the signals of deconfined matter is determined by the very early stages where a dense strongly off-equilibrium parton system formed. A possible suppression of these very early signals seems to enhance the chance to see more from the quark-gluon plasma and hadron sources of photons [20].

Note however, that our scenario does not cover the full pre-equilibrium stage. Here we consider only the chemical equilibration. We hope to handle the gluon thermalization and subsequent quark admixiture thermalization processes within more general kinetic theory models. In particular one has to address the question whether the still not equilibrated "hot" partons in very early stages enhance the hard (large invariant mass) probes of parton matter, and therefore counter-balance the here discussed suppression of semi-hard probes.

4 Summary

In summary we consider here the chemical quark equilibration in a thermalized gluon-enriched plasma. The infrared regularized lowest order process $gg = q\bar{q}$ rates point to rather slow quark equilibration. The photon yield is suppressed by a factor 0.5 if the initial quark density is about 20%, as inidicated by present estimates. An additional stronger suppression can be caused by gluon phase space suppression, i.e., if gluons are early thermalized but have a reduced density. The higher initial temperature (in comparison with a lateron fully equilibrated quark-gluon plasma) overcompensates the mentioned suppression of the high-energy probes.

Acknowledgements. We would like to thank G. Zinovjev, D. Seibert, M. Thoma and M. Asakawa for stimulating discussions.

References

[1] J. Engels, J. Finberg, K. Redlich, H. Satz, M. Weber: Z. Phys. C42 (1989) 341, T. Hatsuda: Nucl. Phys. **544** (1992) 27c

[2] K. Kajantie, P.V. Landshoff, J. Lindfors: Phys. Rev. Lett. **59** (1987) 2527, K.J. Eskola, K. Kajantie, J. Lindfors: Nucl. Phys. **B323** (1989) 37

[3] L. van Hove, S. Pokorski: Nucl. Phys. **B86** (1975) 243

[4] E. Shuryak: Phys. Rev. Lett. **68** (1992) 3270

[5] X.N. Wang, M. Gyulassy: Phys. Rev. **D44** (1991) 3501

[6] K. Geiger, B. Müller: Nucl. Phys. **B369** (1992) 600

[7] K. Geiger: Phys. Rev. **D46** (1992) 4965, 4986

[8] I. Kawrakow, J. Ranft: preprint UL-HEP-92-08

[9] T.S. Biro, E. van Doorn, B. Müller, M.H. Thoma, X.N. Wang: preprint Duke-TH-93-46

[10] (Eds.) T.C. Awes, F.E. Obenshain, F. Plasil,M.R. Strayer, C.Y. Wong: Proc. Quark Matter 1991, Nucl. Phys. **A544** (1992) 1c

[11] P.V. Ruuskanen: Nucl. Phys. **A544** (1992) 169c

[12] R. Schmidt, J. Schukraft: preprint GSI-92-19

[13] K.H. Kampert al. (WA80 collaboration): preprint IKP-MS-93/0302, talk given at the Spring Meeting of the German Physical Society, Mainz, 26 March 1993

[14] H. Heiselberg, G. Baym, C.J. Pethick, J. Popp: Nucl. Phys. **A544** (1992) 569c
M.H. Thoma: Proc. Inst. Workshop, Hirschegg XXI 1993, (Ed.) H. Feldmeier

[15] H.C. Eggers, J. Rafelski: Int. J. Mod. Phys. **A6** (1991 1061

[16] L. Combridge: Nucl. Phys. **151** (1979) 429

[17] V.V. Klimov: Yad. Fiz. **33** (1981) 1734 [Sov. J. Nucl. Phys. **33** (1981) 934],
H.E. Weldon: Phys. Rev. **D26** (1982) 2789

[18] H. Satz: Nucl. Phys. **A544** (1992) 371c

[19] J. Kapusta, L. McLerran, D.K. Srivastava: Phys. Lett. **B283** (1992) 145

[20] J. Kapusta, P. Lichard, D. Seibert: Phys. Rev. **D44** (1991) 2774

[21] E. Braaten , R.D. Pisarski: Phys. Rev. Lett. **64** (1990) 1338, Nucl. Phys. **B337** (1990) 569

[22] K. Geiger, J.I. Kapusta: preprint Minnesota Oct. 1992
B. Kämpfer, O.P. Pvalenko: Phys. Lett. **B289** (1992) 127

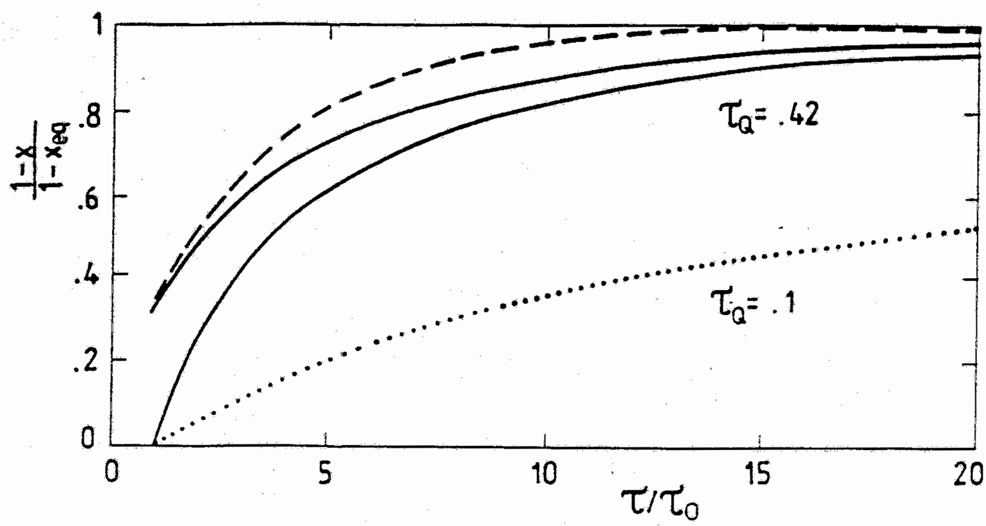

Fig. 1: The time evolution of the relative quark weight $(1-x)/(1-x_{eq})$. The dashed line depicts the evolution in the static case $\gamma = 0$, and the dotted curve is for $\tau_Q = 0.1$. For details consult text.

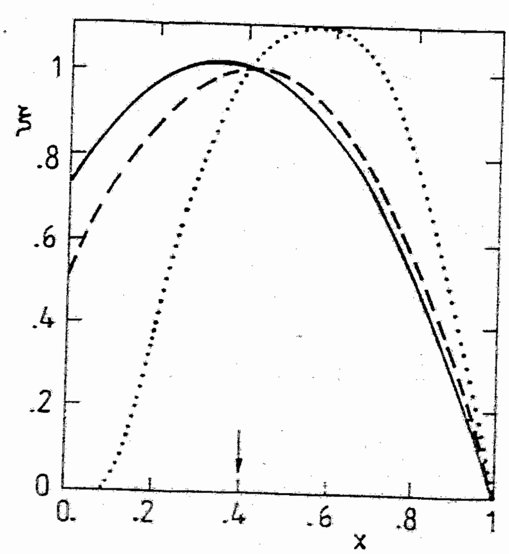

Fig. 2: The ratio of non-equilibrium to equilibrium rates as function of the gluon weight x at $T = 500$ MeV and for $\alpha_s = 0.5$. Full/dashed/dotted curves are for photon energies $E = 3/2/1$ GeV. The arrow indicates the equilibrium value $x_{eq} = 2/5$.

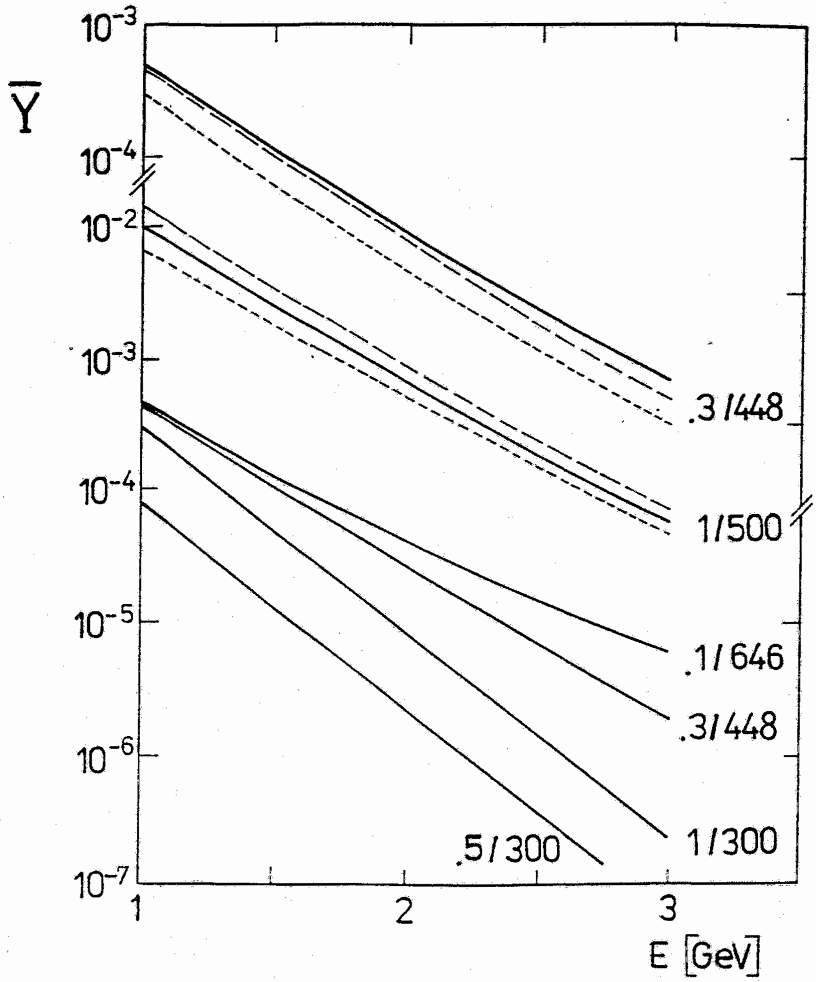

Fig. 3: The scaled photon yield $\bar{Y} = \frac{dN}{dy\, d^3p/E}\left(\pi R^2 \frac{5\alpha\alpha_s n_Q^2}{72^2 T_0^6}\right)^{-1}$ as function of the photon energy E. The curves are labeled by τ_0 (in fm/c) / T_0 (in MeV), and the time integration is extended till reaching T_c = 200 MeV. In the lower part $x = x_{eq}$ is used, and α_s = 0.3/0.5/0.7 for dashed/full/short-dashed curves. The upper part shows the comparison of the yields for different chemical quark equilibrations (dashed/short-dashed lines for τ_Q = 0.5 / $\leq$ 0.1, $x_0 = 0.8$), while the full curve is for $x = x_{eq}$ ($\tau_0 = 0.3$ fm/c, $T_0 = 448$ MeV).